PHYSICAL REVIEW B **79**, 121402(R) (2009)

Dynamics of Ag clusters on complex surfaces: Molecular dynamics simulations

S. Alkis,[1] J. L. Krause,[1] J. N. Fry,[2] and H.-P. Cheng[3,*]
[1]*Department of Chemistry and Quantum Theory Project, University of Florida, Gainesville, Florida 32611, USA*
[2]*Department of Physics, University of Florida, Gainesville, Florida 32611, USA*
[3]*Department of Physics and Quantum Theory Project, University of Florida, Gainesville, Florida 32611, USA*
(Received 20 August 2008; revised manuscript received 16 November 2008; published 20 March 2009)

We study the diffusion of silver nanoparticles on self-assembled monolayers (SAMs). Silver clusters Ag_n of sizes $n=55$, 147, and 1289 were evolved in contact with an alkanethiol (12 carbon, dodecanethiol) SAM deposited on a gold (111) surface. Analysis based on classical molecular dynamics simulations reveals that these systems exhibit a rich variety of behaviors, from superdiffusive for the lightest cluster to pinned for the heaviest, evolution self-similar in lengths and times for the lightest cluster but with characteristic time scales and directional anisotropies emerging for the heavier clusters.

DOI: 10.1103/PhysRevB.79.121402 PACS number(s): 68.35.Fx, 61.46.−w, 36.40.Sx

Intense investigation of metal-organic interfaces over the past decade has uncovered a vast range of applications in nanomolecular electronics[1–4] and as electrochemical and optical biosensors.[5–9] Diffusion of nanoparticles at such interfaces is of fundamental importance in the making of functional nanostructures. Unlike diffusion on solid surfaces, which has been studied thoroughly (see Refs. 10–12, and additional references therein), the motion of particles on organic molecular surfaces has yet to be explored and offers new possibilities for observing complex phenomena.

Meanwhile, metal clusters, especially noble metals such as Au and Ag, are the most popular candidates for constructing 2D quantum-dot arrays.[13–17] Small metal clusters have interesting spectroscopic properties that are different from those of their bulk counterparts, and they can also be used to immobilize large molecules such as proteins.[18,19] An expectation is emerging that one can utilize special features of nanostructured matter in future technology. Growing nanosize clusters on surfaces can be traced back to the early 1990s. There have been two basic experimental techniques: one that involves size-selected clusters preformed in a chamber and beamed down at the surface and a second that employs self-assembly methods in which clusters form on the surface (see Refs. 13 and 20, and additional references therein). Theoretical investigations in the early to mid-1990s attempted to understand the control mechanisms of the deposition process.[21,22] Since the mid-1990s, studies of nanostructured entities have attracted immense attention, and much effort has been made to create structures with characteristic sizes in the range of 1–100 nm.

One motivation for investigating metal clusters on organic surfaces is to control the interface of metal-organic-metal junctions. In contrast to generating nanodot arrays, the idea is to force metal atoms to coalesce in a controlled way. Because of the strong cohesive energy between metal atoms, and between metal and inorganic materials (silicon, etc.), metal clusters on surfaces must be passivated by organic molecules or separated by an inactive matrix. For gold and silver clusters, molecules with thiol groups are often used to passivate the cluster surfaces.[14–16] A natural alternative is to passivate the bulk surface instead of the clusters. Self-assembled monolayers (SAMs) of alkanethiol on Au(111) surfaces are particularly widely used in surface studies because they are structurally simple, thermodynamically stable, and have well-defined order.[23–26] This system continues to provoke research activity.[27] Previous studies found that atomic diffusion through organic layers prevents the formation of a quality junction.[28]

Controlled deposition or growth of unpassivated metal clusters over organic surfaces would provide a different way of creating nanoparticle arrays or growth of metal-organic-metal junctions. For this purpose, understanding diffusion of atoms and nanoclusters on organic assemblies is of essential importance. We therefore choose this system for our study.

In a recent paper, we presented an extensive investigation of the dynamics and thermodynamics of alkanethiol monolayers[26] on surfaces and the properties of such monolayers in the presence of guest molecules. In this work, using a similar molecular dynamics (MD) simulation method, we focus on the dynamics of silver clusters Ag_n, with $n=55$, 147, and 1289, deposited on alkanethiol monolayers self-assembled on Au(111) surfaces. Clusters with 55 and 147 atoms, known as magic number clusters, are highly stable complete-shell Mackay icosahedra that remain rigid at the simulation temperature. To get the initial configurations we started with geometries that have Mackay icosohedral symmetry with nearest distance of close to that in bulk silver. Structural relaxations were performed at room temperature and then at 150 K before they were placed on the surface. For the 1289 atom cluster, structure relaxation leads to the formation of additional facets and the loss of high symmetry, but the overall shape does not change. The detailed, atom-by-atom structure of a cluster with this size is not an important factor in the physics we present in this Rapid Communication. Metal-metal interactions follow the Sutton-Chen[29] potential, the nonbonding van der Waals (VDW) interactions are described with the universal force field (UFF),[30] Au-S interactions are of a Lennard-Jones (LJ) form obtained from the work of Sellers *et al.*,[31] and the intramolecular interactions for the alkanethiol molecules were described with the Dreiding force field.[32] The choice and validation of these potentials were discussed thoroughly in our previous work.[26] The MD unit box has the shape of a hexagonal $(\sqrt{3}\times\sqrt{3})R30°$ lattice in the x and y directions. In the lateral direction each layer consisted of $18\times15=270$ atoms, with a

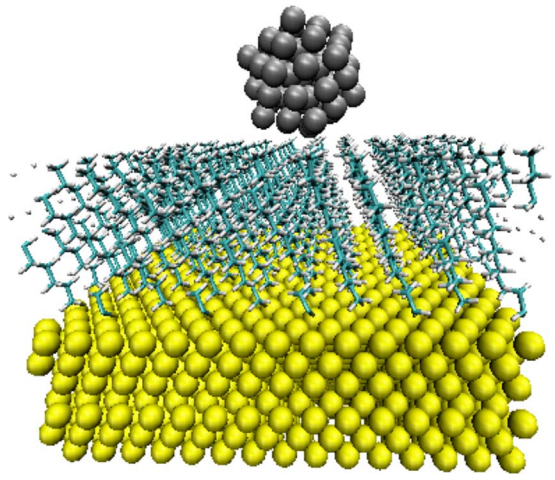

FIG. 1. (Color online) Typical cluster or alkanethiol SAM or gold surface configuration for the $n=55$ cluster. The x direction is oriented left-right in the picture, the y direction is in and out of the page, and the z direction is vertical.

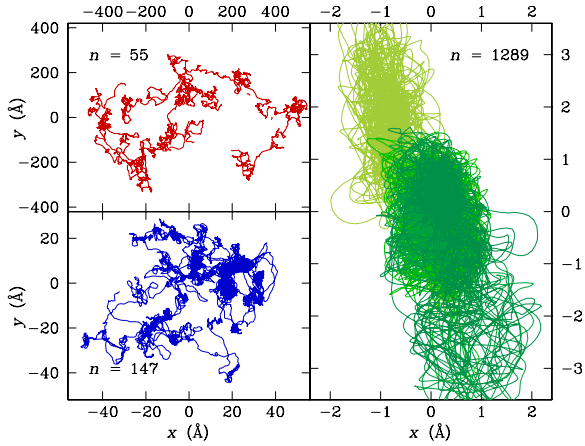

FIG. 2. (Color online) Projected x-y trajectories of cluster center of mass for Ag_n clusters with $n=55$, 147, and 1289 atoms (counterclockwise from top left). For $n=1289$, darker colors are later in time.

size of 44.9 Å by 43.2 Å. The gold atoms were held fixed during the simulations. Ninety alkanethiol molecules were placed on the surface for 100% coverage. Periodic boundary conditions were used in all three directions. A 20 Å vacuum was inserted between two adjacent slabs in the z direction to model the (111) surface. To follow the diffusion of bigger clusters (147 and 1289 atoms) we used a surface four times larger.

The clusters ($n=55$, 147, and 1289) were placed on dodecanethiol SAMs (the closest distance between Ag and alkanethiol atoms was about 3 Å). The systems were relaxed at 0 K during a 10 ns (4 ns equilibration time) simulation. The binding energies of these clusters to the surface (total energy of the system minus the energy of cluster and surface in isolation) are 0.20 eV for the smallest one, 0.22 eV for the midsize one, and 0.61 eV for the largest cluster. After the relaxation, simulations were performed at 150 K to investigate diffusion and sintering; the constant number, volume, and temperature (*NVT*) ensemble Berendsen *et al.*[33] thermostat was used to maintain a constant temperature. This temperature was chosen because at higher temperatures all but the largest cluster are unbound and fly away from the surface. For the smallest cluster we obtained 130 ns of simulation time (in all simulations the first 10 ns of simulation includes 4 ns of equilibration time). For the midsize cluster the total simulation time was 80 ns, and for the largest cluster, the total simulation time was 70 ns. In a test of sintering, we also placed four 55 atom clusters on a surface a factor of 4 larger and ran simulations at 150 K. In this case, the four clusters eventually collided with one another and formed one large cluster. Figure 1 shows a snapshot of a typical simulation configuration, including the gold substrate, the alkanethiol SAM, and a 55 atom cluster.

Figure 2 shows the x-y surface projection of the trajectory of the cluster center of mass for three clusters. The 55 atom cluster trajectory, which lasts 130 ns, is composed of three separate segments, between which the cluster briefly leaves the surface. The 147 atom cluster trajectory covers 80 ns, and the 1289 atom cluster trajectory lasts 70 ns. The trajectories display, in a general sense, a wandering "random walk," but the nature and the scale of the wandering is very different from the smallest to the largest cluster, differences that we quantify in the following analysis. The trajectory is followed as necessary across periodic replications of the simulation volume, an extension that occurs a few times for the intermediate mass cluster and some tens of times for the lightest cluster. This can be done without ambiguity, for example, by integrating the velocity.

All components of velocity are Gaussian distributed to high accuracy for all three clusters, with two-dimensional (2D) x-y variance consistent with the expected $\langle \Delta v^2 \rangle = kT/m$. Measured variances are slightly anisotropic, broader in one direction, and narrower in another. The anisotropy is greatest for $n=1289$, where the excess is $\pm 2.3\%$, only a 2.1-σ effect. However, velocity correlations are very different for different size clusters. Figure 3 shows the spectral densities of the x and y components of the velocity, normalized by the velocity variance. The spectrum of the 55 atom cluster is almost scale free, similar to the characteristic behavior of Brownian motion, for which, as an integral of uncorrelated kicks, the velocity has a f^{-2} spectrum. The spectrum of the 147 atom cluster shows hints of a characteristic scale. The 1289 atom cluster has distinct peaks that are at different frequencies for the x and y components. Insets show the correlation function $c(t)$ of the vector velocity, $c(|t_1 - t_2|) = [\langle \boldsymbol{v}(t_1) \cdot \boldsymbol{v}(t_2) \rangle - \langle \boldsymbol{v}_1 \rangle \cdot \langle \boldsymbol{v}_2 \rangle] / \Delta v_1 \Delta v_2$. All correlations drop sharply, with a time constant of order 0.1 ns or smaller. For the 55 atom cluster the correlation falls off roughly as the exponential of a fractional power, $\exp[-(t/\tau)^\alpha]$, with $\alpha = 0.67 \pm 0.15$ and $\tau = 0.047$ ns. The correlations of the 147 and 1289 atom clusters also show oscillations at multiple frequencies.

Figure 4 shows the root-mean-square displacement $\langle \Delta R^2(t) \rangle^{1/2}$ for two points on a trajectory separated by time difference t and averaged over a trajectory. At small times, the motions of clusters of all sizes are nearly ballistic, $\Delta R = vt$, with $\langle v^2 \rangle = kT/m$ (for $t < 0.01$ ns, the separation be-

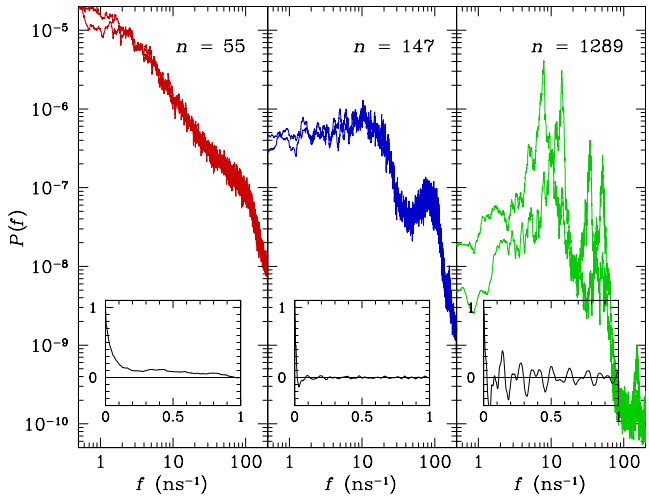

FIG. 3. (Color online) Velocity frequency spectra $P(f)$, normalized by velocity variance, as a function of frequency f. Each panel shows the spectrum for both the x and y components, which are indistinguishable except for $n=1289$. Spectra are smoothed over a moving window of ± 20 points; remaining statistical uncertainties are reflected in the widths of the curves. Insets show the (vector) velocity correlation as a function of time separation t over times from 0 to 1 ns.

haves as $\Delta R \sim t^{\gamma}$ with $\gamma_{55}=0.95$, $\gamma_{147}=0.89$, and $\gamma_{1289}=0.95$). For $n=55$ the late time trajectory has $\Delta R \sim t^{\gamma}$ with a superdiffusive value $\gamma_{55}=0.65$. This scaling applies not only to the root-mean-square ΔR; the entire distribution scales roughly self-similarly. Unlike the power-law distribution found in Ref. 12, the distributions we find for ΔR at a fixed time separation fall off exponentially. For the 1289 atom cluster and for $t>0.1$ ns the cluster sticks in place; $\Delta R(t)$ grows almost not at all, approximately logarithmically, with many oscillations apparent. The $n=147$ cluster presents an intermediate behavior, approximately Brownian, with $\gamma=0.43$. None of these

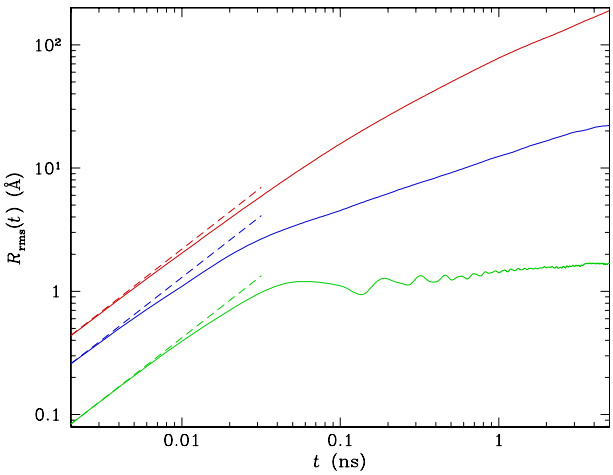

FIG. 4. (Color online) Root-mean-square displacement $\langle \Delta R^2(t) \rangle^{1/2}$ averaged over a trajectory as a function of time t for $n=55$, $n=147$, and $n=1289$ (top to bottom). Dashed lines show the ballistic limit $R=vt$ for thermal velocity $\langle v^2 \rangle = kT/m$; for small times the motion is nearly ballistic.

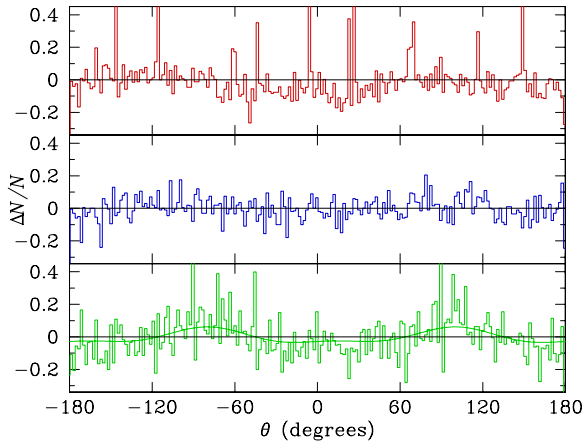

FIG. 5. (Color online) Velocity anisotropy: histogram of fractional deviation from isotropy for velocity as a function of direction for $n=55$, $n=147$, and $n=1289$ (top to bottom). Deviations are small, and with similar numbers of points all bins have similar uncertainties, reflected in the bin-to-bin scatter.

exhibit the stick/flight bifurcation found in Ref. 12.

Figure 5 shows the distribution of fractional departures from isotropy in the velocity direction as a function of orientation. Several of the tallest spikes in the distribution for $n=55$ represent extended times when the cluster is not strongly in contact with the surface. Writing $f(\theta)=\Delta N/N$ as a series in $\sin m\theta$ and $\cos m\theta$, we find no statistically significant anisotropy for $n=55$ or $n=147$, but for $n=1289$ there is a significant (5.75-σ) $m=2$ mode, with amplitude 0.043 peaked along the axis $\theta=98.5°$ and $\theta=-81.5°$. This is approximately the direction in which the trajectory is extended in Fig. 2. The curve in the figure includes this $m=2$ mode plus a marginally significant $m=4$ (2.37-σ) (a higher significance than any mode for either of the other two clusters) that makes the contrast between highest and lowest probabilities to be about 8.8%.

Based on these quantitative statistics and on visualizations of the evolution, we have developed the following picture. All clusters display a nearly ballistic motion for time intervals shorter than a few hundred picoseconds. For longer times, longer than about 1 ns, the lightest cluster continues to move freely over the alkanethiol layer, sliding or rolling over the ends of alkanethiol strands in a motion resembling the activity known as crowd surfing at a concert or sporting event, but with a slightly impeded motion as the alkanethiol strands tug at the surface of the cluster. The motion of the heaviest cluster is much more substantially impeded, resembling that of a tethered balloon buffeted by gusts of wind. The frequency spectra reflect this, with a featureless directionally isotropic spectrum for the $n=55$ cluster, but with pronounced spectral peaks at characteristic scales, different for the x and y components of the motion for the $n=1289$ cluster. The behavior of the $n=147$ cluster lies in between all of these considerations. From the smallest to the largest cluster, the low-frequency power components decrease substantially from one to the next.

In conclusion, we have developed a theoretical understanding of nanosize particle motion on organic assemblies

based on large-scale simulations that include a huge number of degrees of freedom. Unlike motions on solid surfaces, nanosilver particles on organic surfaces can display size-dependent non-Brownian motions. Our analysis of the transition from superdiffusive motion to localized vibration can apply to a wide range of particle motions on organic surfaces with different sizes. Further work is underway to study temperature effects and effects of the strength of the interactions between the particle and the substrate.

We have found visual examination of the evolution to be of value in our analysis. Animations are available on the web.[34]

We have benefited from useful discussions with J. Shen at Oak Ridge National Laboratory and N. Kebaili at Université Paris-Sud. This work was supported by the DOE under Grants No. DE-FG02-97ER45669 and No. DE-FG02-02ER45995 (H.-P.C.).

*Corresponding author; cheng@qtp.ufl.edu

[1] Z. H. Xiong, D. Wu, Z. V. Vardeny, and J. Shi, Nature (London) **427**, 821 (2004).
[2] H. B. Akkerman, P. W. M. Blom, D. M. de Leeuw, and B. de Boer, Nature (London) **441**, 69 (2006).
[3] Y. Selzer, L. T. Cai, M. A. Cabassi, Y. X. Yao, J. M. Tour, T. S. Mayer, and D. L. Allara, Nano Lett. **5**, 61 (2005).
[4] *Molecular Nanoelectronics*, edited by M. A. Reed and T. Lee (American Scientific, Stevenson Ranch, 2003).
[5] N. K. Chaki and K. Vijayamohanan, Biosens. Bioelectron. **17**, 1 (2002).
[6] Th. Wink, S. J. van Zuilen, A. Bult, and W. P. van Bennekom, Analyst (Cambridge, U.K.) **122**, R43 (1997).
[7] D. J. Maxwell, J. R. Taylor, and S. M. Nie, J. Am. Chem. Soc. **124**, 9606 (2002).
[8] C. M. Niemeyer and C. A. Mirkin, *Nanobiotechnology: Concepts, Applications, and Perspectives* (Wiley-VCH, Weinheim, 2004).
[9] C. A. Mirkin and C. M. Niemeyer, *Nanobiotechnology II: More Concepts and Applications* (Wiley-VCH, Weinheim, 2007).
[10] *Surface Diffusion: Atomistic and Collective Processes*, Nato Advanced Studies Institute, Series B: Physics, edited by M. C. Tringides (Plenum, New York, 1997), Vol. 360.
[11] M. C. Tringides and Z. Chvoj, *Collective Diffusion on Surfaces: Correlation Effects and Adatom Interactions* (Kluwer Academic, Dordrecht, 2001).
[12] W. D. Luedtke and U. Landman, Phys. Rev. Lett. **82**, 3835 (1999).
[13] K.-H. Meiwes-Broer, *Metal Clusters at Surfaces: Structure, Quantum Properties, Physical Chemistry* (Springer, Berlin, 2000).
[14] M. J. Tarlov, Langmuir **8**, 80 (1992).
[15] M. J. Hostetler *et al.*, Langmuir **14**, 17 (1998).
[16] P. Mulvaney, Langmuir **12**, 788 (1996).
[17] S. H. Chen, Z. Y. Fan, and D. L. Carroll, J. Phys. Chem. B **106**, 10777 (2002).
[18] R. E. Palmer, S. Pratontep, and H. G. Boyen, Nature Mater. **2**, 443 (2003).
[19] C. Leung, C. Xirouchaki, N. Berovic, and R. E. Palmer, Adv. Mater. (Weinheim, Ger.) **16**, 223 (2004).
[20] P. Jena, S. N. Khanna, and B. K. Rao, *Clusters and Nanoassemblies: Physical and Biological Systems* (World Scientific, Singapore, 2005).
[21] H.-P. Cheng and U. Landman, Science **260**, 1304 (1993).
[22] H.-P. Cheng and U. Landman, J. Phys. Chem. **98**, 3527 (1994).
[23] C. A. Widrig, C. Chung, and M. D. Porter, J. Electroanal. Chem. Interfacial Electrochem. **310**, 335 (1991).
[24] L. H. Dubois, B. R. Zegarski, and R. G. Nuzzo, J. Chem. Phys. **98**, 678 (1993).
[25] D. M. Alloway, M. Hofmann, D. L. Smith, N. E. Gruhn, A. L. Graham, R. Colorado, V. H. Wysocki, T. R. Lee, P. A. Lee, and N. R. Armstrong, J. Phys. Chem. B **107**, 11690 (2003).
[26] S. Alkis, P. Jiang, L. L. Wang, A. E. Roitberg, H.-P. Cheng, and J. L. Krause, J. Phys. Chem. C **111**, 14743 (2007).
[27] A. Cossaro, R. Mazzarello, R. Rousseau, L. Casalis, A. Verdini, A. Kohlmeyer, L. Floreano, S. Scandolo, A. Morgante, M. L. Klein, and G. Scoles, Science **321**, 943 (2008).
[28] W. Xu, G. J. Szulczewski, P. Leclair, I. Navarrete, R. Schad, G. Miao, H. Guo, and A. Gupta, Appl. Phys. Lett. **90**, 072506 (2007).
[29] A. P. Sutton and J. Chen, Philos. Mag. Lett. **61**, 139 (1990).
[30] A. K. Rappé, C. J. Casewit, K. S. Colwell, W. A. Goddard, and W. M. Skiff, J. Am. Chem. Soc. **114**, 10024 (1992).
[31] H. Sellers, A. Ulman, Y. Shnidman, and J. E. Eilers, J. Am. Chem. Soc. **115**, 9389 (1993).
[32] S. L. Mayo, B. D. Olafson, and W. A. Goddard, J. Phys. Chem. **94**, 8897 (1990).
[33] H. J. C. Berendsen, J. P. M. Postma, W. F. van Gunsteren, A. DiNola, and J. R. Haak, J. Chem. Phys. **81**, 3684 (1984).
[34] http://www.qtp.ufl.edu/cheng/animation/dancing_cluster/